Sensors and Materials, Vol. 38, No. 6 (2026) 2995–3004
MYU Tokyo

S & M 4482

Electrochemical Kinetic Modeling of Interfacial Aptamer–Cardiac Troponin I Binding via Cyclic Voltammetry

Seung Jun Jung and Jin-Won Park*

Department of Chemical and Biomolecular Engineering, College of Energy and Biotechnology,
Seoul National University of Science and Technology,
232 Gongneung-ro, Nowon-gu, Seoul 01811, Republic of Korea

(Received March 12, 2026; accepted April 30, 2026)

Keywords: cardiac troponin I, aptamer, cyclic voltammetry, kinetic modeling

In this study, we present a kinetic investigation of interfacial cardiac troponin I (cTnI)-aptamer interactions using cyclic voltammetry (CV). An aptamer-complementary strand complex immobilized on a gold electrode was employed as a model system to examine the concentration-dependent adsorption behavior of cTnI. CV measurements with respect to the interaction time revealed that the interaction process follows pseudo-first-order kinetics under constant surface coverage conditions. By correlating charge variation with fractional surface occupation, an interaction rate constant (k) was derived from the kinetic model. A strong power-law relationship (R^2 = 0.9515) between cTnI concentration and the derived rate constant was established, demonstrating a predictable concentration-dependent detection.

1. Introduction

Troponin is a core protein complex of thin filaments, which regulates the contraction of skeletal and heart muscles.(1) This complex coordinates the basic mechanism activity by playing a decisive role in linking changes in intracellular calcium ion concentration and the occurrence of muscle contraction.(2) The troponin complex consists of three subunits: troponin C (TnC), which is a Ca^{2+} binding site, troponin I (TnI), which inhibits actin–myosin interaction, and troponin T (TnT), which is a tropomyosin binding site.(1) Ca^{2+}-dependent muscle contraction regulation is achieved through their structural and biochemical interactions. Cardiac troponin I (cTnI) and cardiac troponin T (cTnT), which are expressed in the heart muscle, are distinct from skeletal muscle isomorphic proteins in their structures and metabolic characteristics and act as key regulators of heart function.(3) Understanding the physiological roles of cardiac troponin is essential for understanding not only the normal function of the myocardium but also the mechanism by which it develops various cardiomyopathies.(2)

When myocardial cells are damaged, cardiac troponins are released into the bloodstream. Owing to their high specificity and sensitivity to heart injury, they have been widely used as

*Corresponding author: e-mail: jwpark@seoultech.ac.kr
https://doi.org/10.18494/SAM6331

ISSN 0914-4935 © MYU K.K.

gold-standard biomarkers for the diagnosis of cardiovascular diseases including acute myocardial infarction (AMI) for the past 25 years. Consequently, the accurate and rapid measurement of cardiac troponin concentration is critical for early diagnosis, prognosis prediction, and timely clinical decision-making. To date, standard troponin detection methods have primarily relied on immunochemical diagnostics based on specific antibody–antigen interactions, such as enzyme-linked immunoassay (ELISA), surface plasmon resonance (SPR), and fluorescence-based immunoassay.[4–6] Although these techniques provide excellent analytical performance, they typically require complex labeling or washing procedures, expensive instrumentation, and relatively long assay times to inhibit rapid and simple analysis.

Aptamers have emerged as promising alternatives to antibodies as molecular recognition elements and are synthetically produced with high batch-to-batch reproducibility, enhanced chemical stability, and flexible surface immobilization strategies.[7,8] These advantages have led to increasing interest in aptamer-based biosensors (aptasensors) for cardiac troponin detection. Electrochemical aptasensors have attracted significant attention owing to their low cost, portability, rapid response, and compatibility with miniaturized sensing platforms.[9–12] Feng et al. reported a label-free electrochemical adenosine sensor based on target-induced aptamer displacement.[13] However, despite these advantages, many reported electrochemical aptasensors still rely primarily on endpoint or saturated signal measurements. Such approaches often require relatively long interaction times to reach equilibrium and do not fully exploit the kinetic information inherent in the aptamer-target binding process, thereby limiting their usefulness for rapid quantitative analysis.

Cyclic voltammetry (CV) is one of the most fundamental electrochemical techniques for probing interfacial electron transfer processes and surface-confined reactions. By linearly sweeping the electrode potential in forward and reverse directions, CV provides characteristic current-potential responses that are highly sensitive to changes in surface charge and electron transfer behavior.[14–18] Owing to its simple experimental configuration, label-free detection capability, and strong sensitivity to surface modifications, CV has been widely employed in electrochemical sensing applications, including affinity-based protein detection.[19,20] Compared with other electrochemical techniques, CV enables the direct and intuitive evaluation of surface-confined charge transfer processes, making it particularly suitable for the kinetic analysis of biomolecular interactions occurring at electrode interfaces.

In this study, we investigated the concentration-dependent kinetics of the interaction between an aptamer-complementary strand complex immobilized on a gold electrode and cTnI using cyclic voltammetry. Rather than relying on conventional saturated binding signals, we focus on the interaction process and derive the interaction rate constant as a new quantitative indicator. By establishing a functional relationship between cTnI concentration and the interaction rate constant, in this work, we propose a time-efficient and predictive strategy for rapid and sensitive cTnI quantification. This approach provides a crucial technological foundation for the development of high-speed aptamer-based point-of-care testing.

2. Materials and Methods

2.1 Aptamer immobilization

The aptamer sequence targeting cTnI was 5'-CGTGCAGTACGCCAACCTTTCTCATGCG-CTGCCCCTCTTA-3'.[9,21] The aptamer-complementary strand complex was prepared by annealing this sequence with its complementary strand, which was modified with a thiol-C6 functional group at its 5' end for immobilization onto the gold surface. Chemical reagents are tris(2-carboxyethyl)phosphine hydrochloride (TCEP), ethylene diaminetetraacetic acid (EDTA), tris-(hydroxymethyl)aminomethane (Tris-HCl), sodium chloride (NaCl), 6-mercapto-1-hexanol (MCH), potassium hexacyanoferrate(III) ($K_3Fe(CN)_6$), potassium nitrate (KNO_3), and phosphate-buffered saline (PBS, 10 mM). cTnI was purchased from Sigma-Aldrich. All aqueous solutions were prepared using deionized water (distilled water), and ethanol was used for electrode cleaning.

2.2 Cyclic voltammetry measurements

The bare gold electrode was prepared by sequentially polishing its surface with distilled water and ethanol. The electrochemical characteristics of the bare electrode were then verified using CV. The CV measurement was conducted in an electrolyte solution consisting of 5 mM $K_3Fe(CN)_6$ (redox mediator) and 0.1 M KNO_3 (supporting electrolyte). CV was performed over an applied potential range from –200 to 600 mV, and the corresponding current change was recorded to establish a baseline.[22]

A 30 nmol stock of the aptamer-complementary strand complex was diluted into a dedicated hybridization and immobilization buffer to achieve a final concentration of 1 μM.[23,24] The buffer composition was 5 mM TCEP in a solution of 10 mM Tris-HCl, 1 mM EDTA, and 100 mM NaCl (pH 7.4).[25,26] The pretreated gold was immersed in 300 μL of the 1 μM aptamer solution and incubated at room temperature for 2 h. During this period, the thiol-C6 group on the complementary strand forms a self-assembled monolayer, fixing the aptamer onto the electrode surface. This immobilization process was expected to cause a decrease in electrochemical signal (peak current) due to charge hindrance. Following immobilization, the electrode was thoroughly washed with distilled water. CV was performed again using the electrolyte solution to verify the successful aptamer binding based on the observed change in peak current.

Nonspecific binding between the target analyte (cTnI) and any residual bare areas of the gold electrode surface was prevented using MCH. The MCH solution mixed with 5 mM TCEP was prepared with a final concentration of 5 mM. The aptamer-modified electrode was immersed in 300 μL of the 5 mM MCH solution for 1 h at room temperature. The electrode was washed with distilled water and measured via CV to confirm the completion of the blocking step. Figure 1 is a schematic diagram of electrode surface modification. Upon the binding of cTnI, the structural transition induces changes in interfacial charge transfer behavior, which are monitored by cyclic voltammetry.

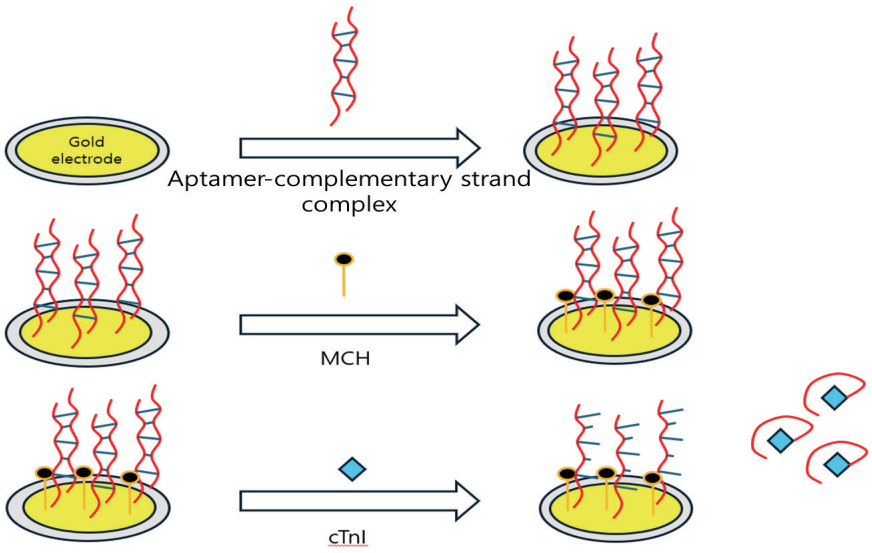

Fig. 1. (Color online) Schematic diagram of aptamer and cTnI interaction on the electrode surface.

The 50 μg stock of cTnI was dissolved in 10 mM PBS and subsequently diluted to a set of target concentrations: 10, 30, 50, 70, and 90 pg/mL. To identify the optimal incubation time, CV was performed while incrementally increasing the interaction time of the aptasensor with a 10 pg/mL cTnI solution. The aptasensor was then exposed to the various cTnI concentrations (10 to 90 pg/mL).

3. Results and Discussion

We observed how the interaction between cTnI and its aptamer changed at a concentration of 10 pg/mL for 20 min to 4 h [Fig. 2(a)]. Since the average charge value was stationary after 2 h, the saturation point was set to 2 h. On the basis of this result, the interactions at different concentrations were measured with respect to the interaction time [Fig. 2(b) on next page]. As a non-target protein control, bovine serum albumin produced CV curves very similar to those of the MCH-blocked electrode, suggesting that nonspecific adsorption contributed only minimally to the observed cTnI response.

The 20 min incubation point was selected for concentration-dependent comparison because it lies in the early kinetic regime before signal saturation, whereas the time-course experiment indicated that the response became nearly stationary after 2 h. Thus, the 20 min data are more suitable for distinguishing concentration-dependent interaction kinetics and for demonstrating the rapid-detection concept of this study. To analyze the kinetics of the binding between cTnI and the aptamer-complementary strand complex, the amount of the charges transferred to the electrode was converted into the fraction of the complex. The fraction was calculated on the basis of the CV result at the saturation point. As shown in Fig. 1, the binding induced the aptamer-complementary strand complex to a single strand, and this induction increased the

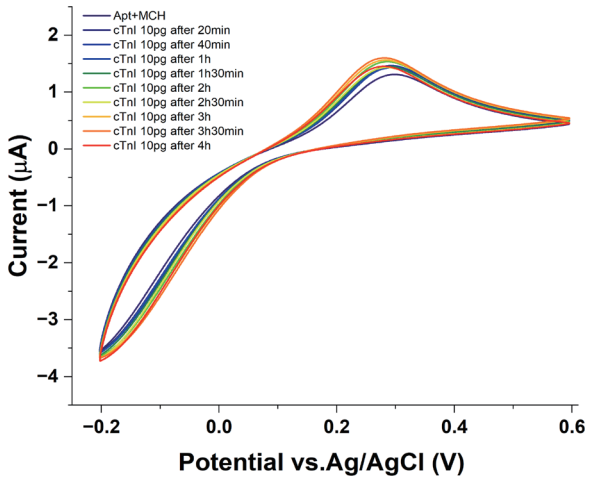

(a)

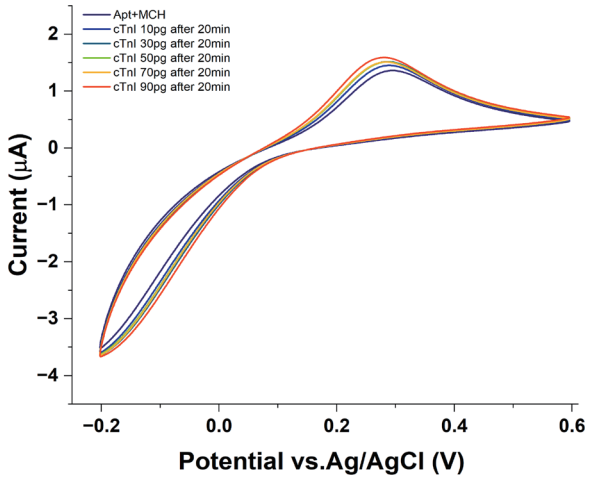

(b)

Fig. 2. (Color online) CV results of interaction between aptamer and cTnI: (a) time-dependent change at cTnI 10 pg/mL and (b) 20 min interaction at different cTnI concentrations.

amount of the transferred charges. Therefore, the generation rate of the binding fraction (θ) was proportional to the available fraction ($1-\theta$) of the binding site where cTnI was able to bind, as pseudo first-order reactions.[27] The rate constant (k) was defined as the proportional constant as below.

$$d\theta/dt = k(1-\theta) \tag{1}$$

$$kt = -\ln(1-\theta) \tag{2}$$

The rate of aptamer conversion into the single strand depended on the concentration of cTnI. The higher the concentration, the higher the amount of charge. Therefore, k was found at each concentration and correlated with the concentration.

Table 1 shows the fraction and the amount of charge transferred to the electrode with respect to the interaction time. The change after the cTnI addition was calculated at each time, and the fraction was calculated by dividing the change at each time by the change at 2 h. Fitting was performed for the fraction with respect to time, as shown in Fig. 3. From the slope of the linear fitting, the rate constant (k) was estimated.

The relationship between the rate constant (k) and the cTnI concentration was investigated. The procedures described above were performed to find the constant for each concentration. The results are summarized in Table 2.

The rate constant (k) was found as 0.64-power of the cTnI concentration, as shown in Fig. 4 with a determination coefficient (R^2) of 0.9515. The concentration-dependent data were obtained from [n = 4] independent measurements, and the error bars in Figs. 4 and 5 represent average ±15%.

Table 1
Relationship between charge and fraction with respect to time at cTnI 10 pg/mL.

Time (min)	Charge (μQ)	Charge change (μQ)	Fraction (θ)	$-\ln(1-\theta)$
0	25.64	0	0	0
20	27.40	1.63	0.51	0.72
40	27.65	2.01	0.58	0.88
60	27.13	1.49	0.43	0.57
90	27.67	2.03	0.59	0.90
120	29.01	3.37	0.98	4.00

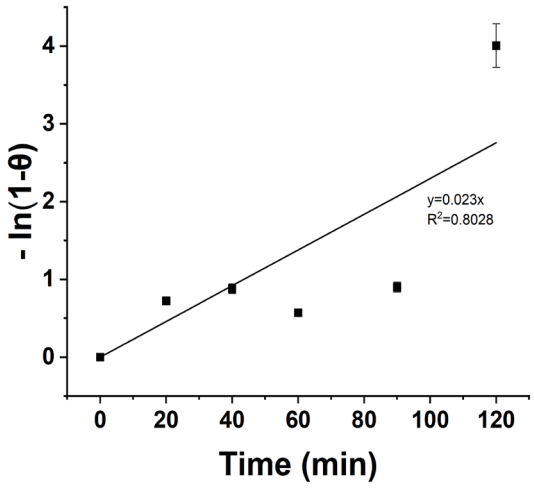

Fig. 3. Relationship between time and fraction at cTnI 10 pg/mL.

Table 2
Results of fraction and charge at different concentrations for 20 min interaction time.

Concentration (pg/mL)	Charge change (μQ)	Fraction (θ)	$-\ln(1-\theta)$	k (min^{-1})
10	1.63	0.48	0.65	0.03
30	2.29	0.67	1.11	0.06
50	2.69	0.78	1.53	0.08
70	2.99	0.87	2.04	0.10
90	3.23	0.94	2.83	0.14

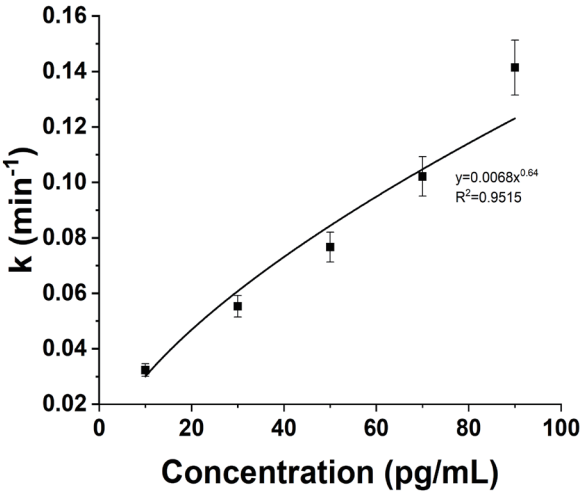

Fig. 4. Relationship between rate constant (k) and cTnI concentration.

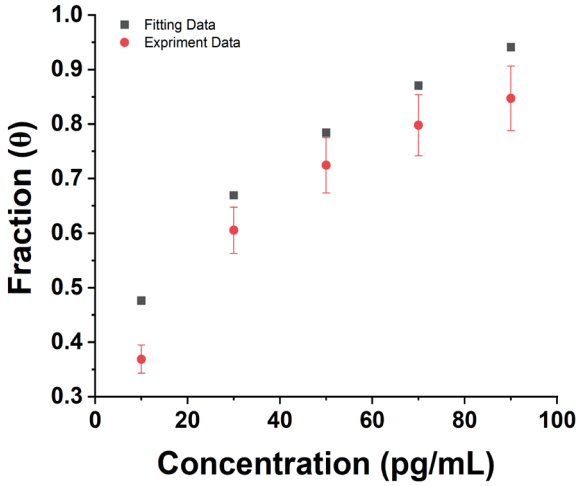

Fig. 5. (Color online) Comparison between fitting and experimental data at each cTnI concentration. The squares indicate the fitted fraction and the circles indicate the experimental fraction.

The fraction at each concentration was calculated from the fitting relation and compared with the experimental results. In Fig. 5, the squares and circles indicate the fitting and experimental results, respectively, which show similarity with each other.

The kinetic behavior observed in this study reflects the interplay between bulk transport and surface reaction mechanisms. Because the aptamer layer is immobilized as a self-assembled monolayer on gold, the available binding sites are spatially confined. The pseudo-first-order model assumes that surface coverage is sufficiently low during initial interaction such that the number of available sites remains effectively constant relative to bulk concentration. The observed power-law relationship suggests that the overall adsorption rate is governed by a combination of reaction-controlled and diffusion-influenced processes. At low concentrations, the adsorption rate is likely reaction-limited, whereas at high concentrations, local mass transport effects may contribute to deviations from the ideal first-order behavior.

The accurate and rapid measurement of cTnI concentration is essential for the diagnosis of AMI and rapid treatment determination. The clinical concentration, which is the criterion for AMI diagnosis, that is, the upper reference limit of the 99th percentile of the high-sensitivity cTnI (hs-cTnI) assay is reported as 18 ng/L (18 pg/mL) for the Korean health reference group.[28] The cTnI concentration range considered in this research is well matched for the clinical one. The modeling framework presented here provides a systematic approach for extracting adsorption rate constants from electrochemical measurements, which may support the future development of rapid electrochemical assays. Unlike equilibrium-based analysis, this method emphasizes the quantitative comparison of concentration-dependent interaction kinetics in surface-confined biomolecular systems.

4. Conclusions

In this study, we presented a kinetic analysis of interfacial aptamer–protein interactions using cyclic voltammetry. The electrochemical measurements with respect to the interaction time demonstrated that the interaction process follows a pseudo-first-order kinetic model under constant surface immobilization conditions. By correlating charge variation with fractional surface occupation, interaction rate constants were derived for different bulk concentrations. A strong power-law relationship between concentration and the extracted rate constant (R^2 = 0.9515) was established, confirming the predictable dependence of the interaction on analyte concentration. The proposed modeling framework provides a systematic approach for analyzing surface-confined reaction processes and may be extended to other functionalized electrochemical interfaces.

Acknowledgments

This study was supported by the Research Program funded by SeoulTech (Seoul National University of Science and Technology).

References

1 V. L. Filatov, A. G. Katrukha, T. V. Bulargina, and N. B. Gusev: Biochemistry (Moscow) **64** (1999) 969. http://protein.bio.msu.ru/biokhimiya/contents/v64/full/64091155.html
2 I. A. Katrukha: Biochemistry (Moscow) **78** (2013) 1447. https://doi.org/10.1134/S0006297913130063
3 A. M. Chaulin: Biology **11** (2022) 429. https://doi.org/10.3390/biology11030429
4 H. Ma, A. Cassedy, and R. O'Kennedy: J. Immunol. Methods **497** (2021) 113108. https://doi.org/10.1016/j.jim.2021.113108
5 J. Homola: Chem. Rev. **108** (2008) 462. https://doi.org/10.1021/cr068107d
6 R. Radha, S. K. Shahzadi, and M. H. Al-Sayah: Molecules **26** (2021) 4812. https://doi.org/10.3390/molecules26164812
7 S. P. Song, L. H. Wang, J. Li, J. L. Zhao, and C. H. Fan: TrAC Trends Anal. Chem. **27** (2008) 108. https://doi.org/10.1016/j.trac.2007.12.004
8 I. Palchetti and M. Mascini: Anal. Bioanal. Chem. **402** (2012) 3103. https://doi.org/10.1007/s00216-012-5769-1
9 H. Jo, H. Gu, W. Jeon, H. Youn, J. Her, S. K. Kim, J. Lee, J. H. Shin, and C. Ban: Anal. Chem. **87** (2015) 9869. https://doi.org/10.1021/acs.analchem.5b02312
10 J. Ma, L. Feng, J. Li, D. Zhu, L. Wang, and S. Su: Biosensors **13** (2023) 746. https://doi.org/10.3390/bios13070746
11 J. Li, S. Zhang, L. Zhang, Y. Zhang, H. Zhang, C. Zhang, X. Xuan, M. Wang, J. Zhang, and Y. Yuan: Front. Chem. **9** (2021) 680593. https://doi.org/10.3389/fchem.2021.680593
12 J. F. Zhang, K. Sun, J. T. Ren, H. Wang, and J. Cheng: Sens. Actuators, B **401** (2024) 135001. https://doi.org/10.1016/j.snb.2023.135001
13 Y. Feng, Y. Wang, Y. Zhao, Z. Li, H. Chen, X. Zhang: Electrochem. Commun. **10** (2008) 409. https://doi.org/10.1016/j.elecom.2008.01.024
14 D. Grieshaber, R. MacKenzie, J. Vörös, and E. Reimhult: Sensors **8** (2008) 1400. https://doi.org/10.3390/s8031400
15 M. K. Kang and J.-W. Park: Electron. J. Biotechnol. **52** (2021) 30. https://doi.org/10.1016/j.ejbt.2021.04.005
16 M. K. Kang and J.-W. Park: ACS Omega **6** (2021) 14963. https://doi.org/10.1021/acsomega.1c01023
17 M. K. Kang and J.-W. Park: Sens. Mater. **33** (2021) 1749. https://doi.org/10.18494/SAM.2021.3408
18 Y. Park, M. K. Kang, and J.-W. Park: Appl. Sci. **11** (2021) 3660. https://doi.org/10.3390/app11083660
19 N. Elgrishi, K. J. Rountree, B. D. McCarthy, E. S. Rountree, T. T. Eisenhart, and J. L. Dempsey: J. Chem. Educ. **95** (2018) 197. https://doi.org/10.1021/acs.jchemed.7b00361
20 D. Semenova, A. Zubov, Y. E. Silina, L. Micheli, M. Koch, and K. V. Gernaey: Sens. Actuators, B **259** (2018) 945. https://doi.org/10.1016/j.snb.2017.12.088
21 B. Ropii, M. Bethasari, I. Anshori, A. P. Koesoema, W. Shalannanda, A. Satriawan, C. Setianingsih, M. R. Akbar, R. Aditama, F. Fahmi, E. Sutanto, M. Yazid, and M. Aziz: PLoS ONE **19** (2024) e0302475. https://doi.org/10.1371/journal.pone.0302475
22 K. Chen, H. Zhao, Z. Wang, F. Zhou, Z. Shi, S. Cao, and M. Lan: Biosens. Bioelectron. **212** (2022) 114431. https://doi.org/10.1016/j.bios.2022.114431
23 K. Chen, H. Zhao, Z. Wang, F. Zhou, and M. Lan: Sens. Actuators, B **390** (2023) 134044. https://doi.org/10.1016/j.snb.2023.134044
24 S. H. Jalalian, M. Ramezani, N. M. Danesh, M. Alibolandi, K. Abnous, and S. M. Taghdisi: Biosens. Bioelectron. **117** (2018) 487. https://doi.org/10.1016/j.bios.2018.06.055
25 M. Pali and I. I. Suni: Electroanalysis **30** (2018) 2899. https://doi.org/10.1002/elan.201800495
26 Z. B. Liu, H. Y. Zhang, Y. H. Wang, X. Q. Li, Y. M. Zhao, and J. Zhang: J. Nanopart. Res. **15** (2013) 1964. https://doi.org/10.1007/s11051-013-1964-z
27 W. Norde: Adv. Colloid Interface Sci. **25** (1986) 267. https://doi.org/10.1016/0001-8686(86)80012-4
28 M. Ji, H. W. Moon, M. Hur, and Y. M. Yun: Clin. Biochem. **49** (2016) 756. https://doi.org/10.1016/j.clinbiochem.2016.01.027

About the Authors

Seung Jun Jung is a graduate student at Seoul National University of Science and Technology. His research interests are in molecular detection.
(24510217@seoultech.ac.kr)

Jin-Won Park received his B.S. degree from Korea University in 1998 and his Ph.D. degree from Purdue University, USA, in 2005. Since 2010, he has been a professor at Seoul National University of Science and Technology. His research interests are in biomimetic membranes and their applications.
(jwpark@seoultech.ac.kr)